

D17

N79-15605

ANALYSIS OF A VTOL HOVER TASK WITH PREDICTOR DISPLAYS
USING AN OPTIMAL CONTROL MODEL OF THE HUMAN OPERATOR*

Gunnar Johansson** and T. Govindaraj

Department of Mechanical and Industrial Engineering
Coordinated Science Laboratory
University of Illinois
Urbana Illinois 61801

SUMMARY

The influence of different types of predictor displays in a longitudinal VTOL hover task is analyzed in a theoretical study. It has been assumed that pitch angle and position will be presented to the pilot in separate displays namely the artificial horizon and a position display. The predictive information is calculated by means of a Taylor series. The future pitch angle is extrapolated 0.7s ahead and displayed as an additional bar, whereas the position is displayed as an extrapolated path element. This path element is approximated by three straight line segments, i.e., three future position values are calculated with the end point being 2.0s ahead.

From earlier experimental studies it is well known that predictor displays improve human and system performance and result in reduced human workload. In this study, the optimal control model is used to prove this effect theoretically. The status and predictive quantities are considered as separate observed variables. The Taylor series coefficients are incorporated in the observation matrix. Also, rate information included in the movement of the position and pitch angle indication is represented.

Several cases with differing amounts of predictive and rate information are compared. The results show the expected improvements in human and system performance in terms of RMS-values. The strongest influence is caused by the indication of the extrapolated path element, especially the end point. Computed cost gradients and fractions of attention show the relative importance of the individual pieces of displayed information. An optimization of the attention allocation shows a further improvement in system performance in all cases.

* This work was supported in part by the National Aeronautics and Space Administration under NASA-Ames Grant NSG-2119.

** Permanent Address: Research Institute for Human Engineering(FAT)
D-5309 Meckenheim, F. R. Germany

236
PAGE INTENTIONALLY BLANK

I Introduction

Predictor displays have been investigated intensively in laboratory simulations [1]-[5]. It has been found that they improve human and system performance and result in reduced human workload. More recently, predictor displays have been receiving increasing attention (see, e.g., [6]) because the technology of computer graphics has reached a high standard [7] which allows one to implement these displays more easily in real man-machine systems.

During the last few years, an optimal control model of the human operator (see, e.g., [8], [9]) has been applied as a unified methodology for analytical display design and evaluation [10]-[13]. Attitude/director indicator and flight director displays have been considered as examples.

This paper is a contribution to such an analytical display design and evaluation procedure. Different types of predictor displays in a longitudinal VTOL hover task are analyzed theoretically by means of the optimal control model of the human operator. Rather than fitting experimental data, the purpose here is to calculate the expected human and system performance with different display designs. These results are validated by intuitive reasoning by considering earlier experimental results

In the next section, the VTOL hover task is described. The assumed predictor-display layout is explained in Section III. Section IV gives a brief overview of the optimal control model and emphasizes specific considerations for applying this model to the utilization of predictor displays. Finally, the results of a case study are discussed in Section V

II Description of the VTOL Hover Task

The task chosen in this paper concerns the longitudinal motion of a hovering VTOL aircraft. For comparison purposes the task is the same as that in [14] which since then has also been considered in other papers, e.g., [15], [16].

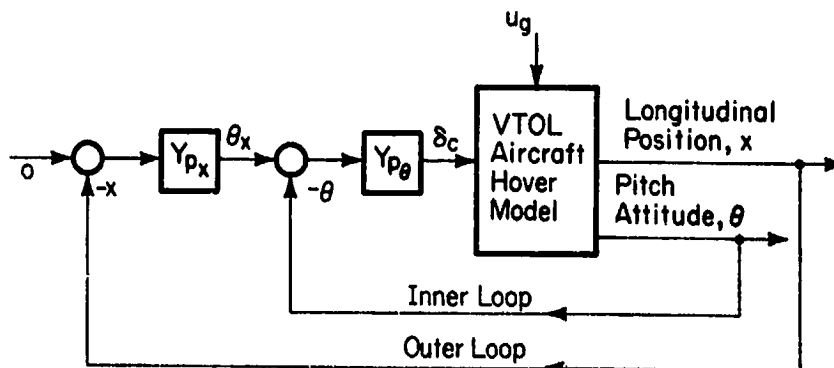


Figure 1: Series Loop Model for Pilot Longitudinal Control in Hover (after [15])

In Equation (1) and Figure 2, g is the gravitational constant and X_u , M_u , M_q , M_δ are aircraft stability derivatives. Their values are chosen to be the same as in the nominal case in [15], namely

$$X_u = 0.1s^{-1}, M_u = 0.0207 \text{ ft}^{-1}s^{-1}, M_q = -3.0s^{-1}, M_\delta = 0.431s^{-2}.$$

Also, the simulated gust is the same as in [15]. The bandwidth of the gust filter is $\omega_b = 0.314 \text{ rad}\cdot\text{s}^{-1}$ and the rms-value of the gust is $u_{g,rms} = 5.14 \text{ ft}\cdot\text{s}^{-1}$, i.e., the variance of the driving white noise is $W_{11} = 16.59$.

III Layout of Assumed Predictor Displays

Two main techniques have been used for generating predictor displays. One is the fast-time model technique [3], [4]; the other one is the extrapolation technique [2], [5]. In this paper, the extrapolation technique is applied. Its advantage is that no model of the aircraft needs to be implemented and run repetitively, faster than real time, to generate predictions on the basis of expected control inputs. Instead, the predictions are calculated by means of a Taylor series on the basis of present measurable position, rate, and acceleration. The only disadvantage of this technique is that it might be difficult to generate noise-free acceleration information, if this is not measurable.

The extrapolation technique is used in the present study to predict extrapolated longitudinal position x as well as pitch angle θ . For position x the predicted value is calculated as follows:

$$x_{PD}(t) = x(t + \tau_x) = x(t) + \tau_x \dot{x}(t) + \frac{\tau_x^2}{2} \ddot{x}(t) \quad (2)$$

The corresponding Taylor series expression for the pitch angle θ reads:

$$\theta_{PD}(t) = \theta(t + \tau_\theta) = \theta(t) + \tau_\theta \dot{\theta}(t) + \frac{\tau_\theta^2}{2} \ddot{\theta}(t) \quad (3)$$

The Taylor series expressions of Equations (2) and (3) are truncated after the second derivative terms. This has been found in earlier experimental studies (see [5]) to be a reasonably good approximation.

It has been assumed, for the longitudinal hover task studied here, that the pilot would view displays with predictive information like those shown in Figure 3. The pitch angle and position information is separately indicated in two displays. The one for the pitch angle or inner loop of Figure 1 is like one dimension of an artificial horizon, whereas the one for the position or outer loop of Figure 1 is presented as a function of time. Similar displays have been studied experimentally in [5] with similar system dynamics, which allows for adopting the following data. A prediction span of

$\tau_e = 0.7s$ seems to be appropriate for pitch. For the position, the indication of an extrapolated path element with a prediction span showing the range between the actual value and the end point (see Figure 3), i.e., $\tau_x = 0...2s$, has been chosen. The curved extrapolated path element can be approximated by, e.g., three straight lines as shown in Figure 3. This reduces the calculation of the path element to that of three points in the future i.e., $(1/3, 2/3, \text{ and } 1) \tau_x$ ahead.

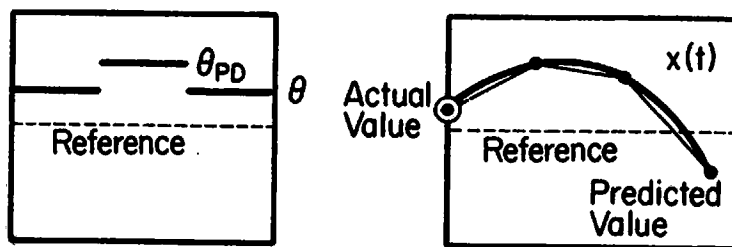


Figure 3: Displays with Predictive Information for Indications of Pitch Angle (left) and Position (right)

IV. Application of the Optimal Control Model

In this paper the same optimal control model for the human operator has been applied as in [15]. In the block diagram of Figure 4, a distinction has been made, however, between influences of display parameters and human perceptual abilities on the observation vector $y(t)$. The human perceptual abilities include (1) estimation in the sense of extracting the first derivative of a displayed variable from its movement as well as (2) perceptual thresholds for the position and rate of displayed variables. For this study all thresholds have been assumed to be zero.

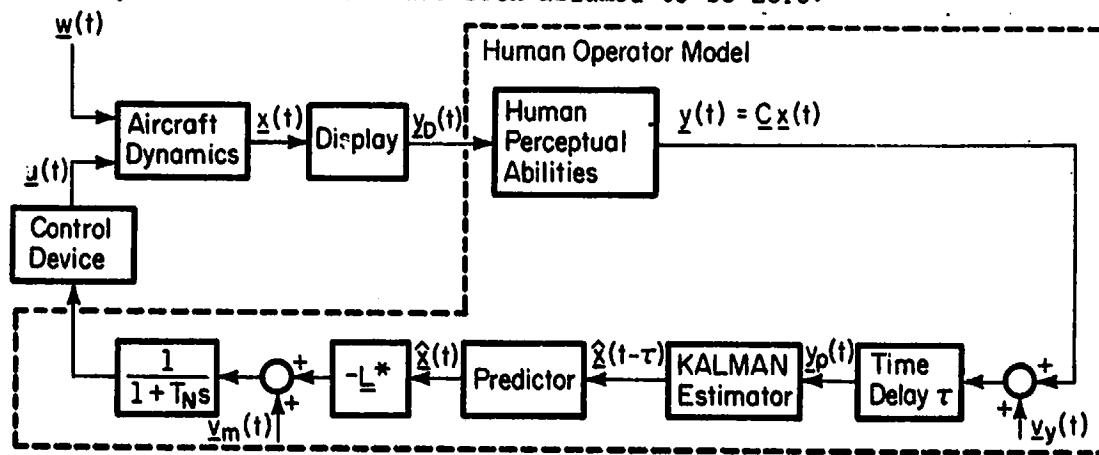


Figure 4: Optimal Control Model for the Human Operator (after [15] and [9])

For reasons of comparing the results of this paper with those of [15], the same parameters of the human operator model and the cost functional have been adopted, whereas the aircraft dynamics are those described by Equation

(1), i.e., having only the very slight change mentioned before. The cost functional for optimal control is

$$J = \overline{x^2} + 400 \overline{q^2} + \tilde{g} \overline{\delta_c^2} \quad (4)$$

i.e., a weighted sum of the mean squared values of the position x , the pitch rate $q = \dot{\theta}$, and the control rate $\dot{\delta}_c$. The time delay of the human operator model is $\tau = 0.15s$, and the lag time constant of the neuromuscular system is adjusted to $T_N \approx 0.1s$ by an appropriate choice of \tilde{g} in Equation (4), i.e., $\tilde{g} = 0.03$. The noise-to-signal ratio of the motor noise is $\rho_m = -25dB$. The noise-to-signal ratios of the observation noises change in this study. However, for the baseline display format with the same observation vector $\underline{y} = [x, u, \theta, q]^T$ as in [15], they are adopted as $\rho_1 = \rho_2 = \rho_3 = \rho_4 = -20dB$.

The described optimal control model should be able to explain the improvements of human and system performance which occur when predictor displays are used. Looking at Figure 3, one can see that all status and predictive information can be described by the following observation vector:

$$\underline{y} = \begin{bmatrix} x \\ u \\ x_{1/3PD} \\ x_{2/3PD} \\ x_{PD} \\ \theta \\ q \\ \theta_{PD} \end{bmatrix} = \underbrace{\begin{bmatrix} 1 & 0 & 0 & 0 & 0 & 0 \\ 0 & 1 & 0 & 0 & 0 & 0 \\ 1 & 1/3\tau_x & 1/18\tau_x^2 & 0 & 0 & 0 \\ 1 & 2/3\tau_x & 2/9\tau_x^2 & 0 & 0 & 0 \\ 1 & \tau_x & 1/2\tau_x^2 & 0 & 0 & 0 \\ 0 & 0 & 0 & 1 & 0 & 0 \\ 0 & 0 & 0 & 0 & 1 & 0 \\ 0 & 0 & 0 & 1 & \tau_\theta & 1/2\tau_\theta^2 \end{bmatrix}}_{\underline{P}} \begin{bmatrix} x \\ \dot{x} \\ \ddot{x} \\ \theta \\ \dot{\theta} \\ \ddot{\theta} \end{bmatrix} \quad (5)$$

which can be expressed in terms of position x and pitch angle θ as well as the first and second derivatives of both variables by applying Equations (2) and (3). The observation vector in Equation (5) considers also rate information, namely $u = \dot{x}$ and $q = \dot{\theta}$ as in the baseline display format, thereby combining the two influences of display parameters and human perceptual abilities of Figure 4.

As the observation vector is normally derived from the state vector, the vector on the right side of Equation (5) composed of position x , pitch angle θ and its first and second derivatives has to be expressed in terms of the state vector. All these components appear in the systems equation (1) and in Figure 2. The mathematical description is:

$$\begin{bmatrix} x \\ \dot{x} \\ \ddot{x} \\ \theta \\ \dot{\theta} \\ \ddot{\theta} \end{bmatrix} = \begin{bmatrix} x \\ \dot{x} \\ \ddot{x} \\ \theta \\ \dot{\theta} \\ \ddot{\theta} \end{bmatrix} = \underbrace{\begin{bmatrix} 0 & 1 & 0 & 0 & 0 & 0 \\ 0 & 0 & 1 & 0 & 0 & 0 \\ X_u & 0 & X_u & -g & 0 & 0 \\ 0 & 0 & 0 & 1 & 0 & 0 \\ 0 & 0 & 0 & 0 & 1 & 0 \\ M_u & 0 & M_u & 0 & M_q & M_\delta \end{bmatrix}}_{\underline{T}} \begin{bmatrix} u_g \\ x \\ u \\ \theta \\ q \\ \delta \end{bmatrix} \quad (6)$$

Taking Equations (5) and (6) together results in the following equation for the observation vector:

$$\underline{y} = \underline{P} \cdot \underline{T} \cdot \underline{x} = \underline{C} \cdot \underline{x} \quad (7)$$

Equation (7) shows that a matrix multiplication is necessary to find the observation matrix C . One of the two matrices being multiplied, i.e., P , reflects the display format and the human perceptual abilities, whereas the other one, i.e., T contains mainly components of the systems matrix A .

In order to investigate the influence of different amount of predictive and rate information, a theoretical case study with the optimal control model has been run. The 13 cases studied differ only in their observation vectors which are chosen as shown in Table I. Available information is denoted by a "1" whereas a "0" means that this component of the observation vector is not present in the corresponding case.

Table I
Composition of the Observation Vectors for the Case Study

	A	B	C	D	E	F	G	H	I	J	K	L	M
x	1	1	1	1	1	1	1	1	1	1	1	1	1
u	1	0	0	1	1	0	0	1	0	0	1	1	0
x _{1/3PD}	0	0	0	0	0	0	0	0	0	1	1	1	1
x _{2/3PD}	0	0	0	0	0	0	0	0	0	1	1	1	1
x _{PD}	0	0	0	0	0	0	0	1	1	1	1	1	1
e	1	1	1	1	1	1	1	1	1	1	1	1	1
q	1	1	0	0	1	1	0	1	0	0	1	1	0
e _{PD}	0	0	0	0	1	1	1	0	0	0	0	1	1

Case L is identical with Equation (5). From this, all others have been derived by omitting a certain amount of information, i.e., deleting the corresponding rows in the observation vector and observation matrix.

Cases A, E, C, and D are concerned with the influence of rate information which has also been investigated in [17]. Case A is the baseline display format of this study and is the same as in [15]. Cases E, F, and G consider only predictive pitch information, whereas cases H, I, J, and K assume only predictive position information, being either only the end point (H,I) or the complete extrapolated path element (J,K). Finally, cases L, M include both predictive pitch and position information.

The case study is carried out using the version of the optimal control model which is described in [18].* This includes an optimization of the fractions of attention the pilot devotes to the individual pieces of displayed information. The optimization technique based on the cost gradients of all pieces of information is described in more detail in [19]. The observation noise-to-signal ratio P_i of the i th observed variable is related to its fraction of attention f_i by

$$P_i = P_0 \frac{1}{f_i} \tag{8}$$

$$\text{with } \sum_i f_i = f_{\text{total}}$$

where P_0 is the full attention noise-to-signal ratio, normally -20 db [10]. Thus the above mentioned noise-to-signal ratios of -20dB for all four

* The authors are grateful to Aerospace Systems, Inc., Burlington, Mass., and William C. Hoffman in particular for furnishing the optimal control model software.

observed variables in the baseline display format correspond to a total attention of 4. The value of 4 is the baseline for full attention and should not be interpreted as the human operator devoting 4 times his full attention to the task.

V Results

Performance scores have been shown in Figures 5 and 6 for all 13 cases. These correspond to a total attention of 4, with attention allocation optimized. RMS-longitudinal and pitch errors have been plotted. They are discussed in some detail here. For both variables, position x and pitch angle θ certain trends are apparent. The error is reduced in all cases when prediction information is presented (cases E-M). There is an increase in RMS-errors when the rate information is not available (without prediction; see cases A-D).

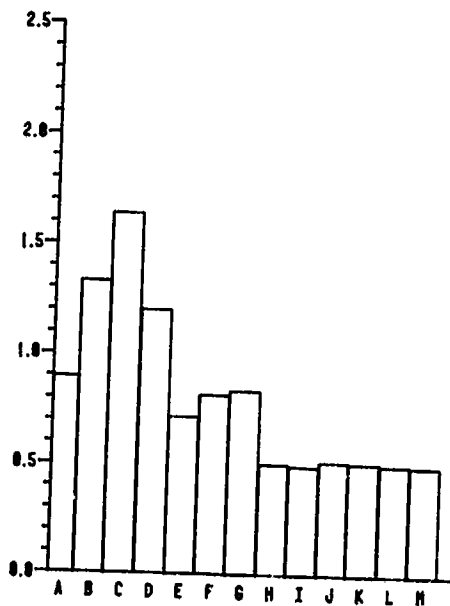


Figure 5: RMS-Longitudinal Errors

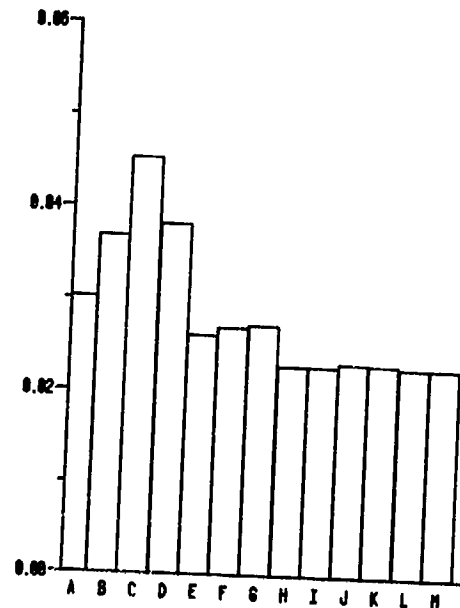


Figure 6: RMS-Pitch Errors

(for all 13 Cases with Optimized Attention Allocation)

For the longitudinal position, the absence of derivative information for position and pitch (C) results in about 80% increase in RMS-error. When only rate u is removed (B), the error increases by about 50%, whereas the increase is only about 33% when the pitch rate is absent (D). Therefore, it is very important that the displays are designed to easily allow the human operator to make good rate estimates.

Compared with the base line performance (A), the reduction in RMS-error is rather small when only the pitch angle predictor is available (E). The error is reduced by about 20%. With predictor information, lack of pitch

rate does not have much effect (see G vs. F), presumably due to the rate information contained implicitly. When rate u is not available (F,G), the RMS-error is reduced only slightly compared with A even when prediction is available for pitch. However, when B and C are compared to F and G respectively, the error is reduced by 35 to 50% with the addition of predictor information.

It is significant to observe that the lack of rate information does not affect the results when the position predictor display is available. This is seen in H and I having nearly equal performance scores. From the baseline performance (A), a reduction in RMS-error of about 45% is observed. It is also important to note that compared to C, the addition of position prediction alone reduces the error to less than 1/3 of its original value. This is validated by intuitive reasoning based on earlier experimental results [5]. With the predictor for a two-dimensional map display, it was found that the lap time, i.e., for one circuit of the map, was reduced by 32%.

When the position predictor is available, all the cases (H-M) result in about the same RMS-errors. This happens irrespective of whether the position and pitch rates and the attitude predictor information are available. This confirms our belief that it is more important to employ predictor display aiding for the slower time constant outer loop. An unexpected result, however, is the fact that additional intermediate points of the extrapolated path element (J-M) do not further improve performance. The most important predictive information seems to be the indication of the end point of the extrapolated path element.

The trends for the pitch angle error are similar to the longitudinal position error. When all derivative information is removed (C), the error increases by about 50%. Absence of u (E) results in a 23% increase, whereas for the pitch rate (D) the corresponding increase is about 30%. The order of B and D is reversed with respect to position error, as could be expected. The pitch angle predictor reduces the error by about 10% (E). Loss of pitch rate information is not important when the predictor is available (G vs. F). These results are in qualitative agreement with earlier experimental results [5], where RMS-errors have been improved by a factor of 2-4 with the addition of a predictor for an artificial horizon in a pure attitude control task. Further reduction in RMS-pitch error, by 23%, occurs when the position predictor display is added (H-M). This is a 50% reduction compared to the no-derivative case (C). As before, no substantial difference occurs if the rate information or intermediate points are removed when the position predictor display is available.

ORIGINAL PAGE IS
OF POOR QUALITY

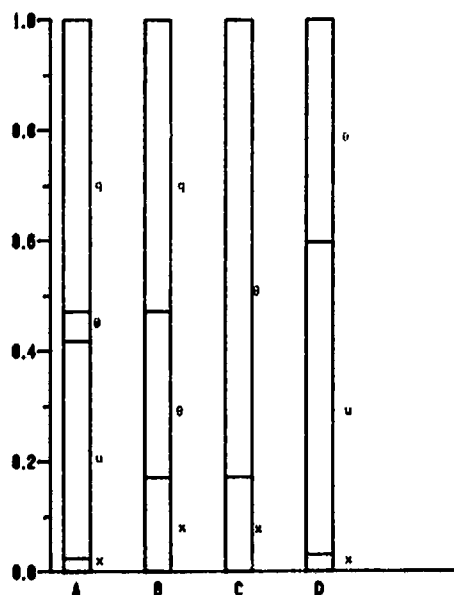


Figure 7: Optimized Fractions of Attention for Cases A B C D

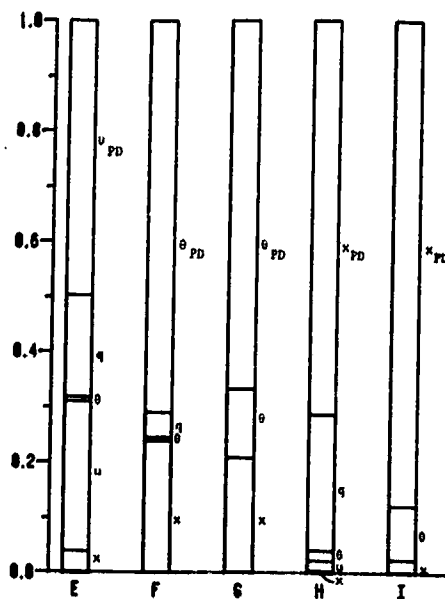


Figure 8: Optimized Fractions of Attention for Cases E F,G H,I

For all 13 cases, the optimized fractions of attention are plotted in Figures 7,8, and 9. The total attention is constant at 4 for all cases, normalized to 1 in the figure, assuming that the human operator will not increase his effort with additionally displayed information. For each displayed variable fractions of attention are shown which result in minimum total cost. When rate information is available, the optimum fraction of attention required is more (mostly by about 8 to 10 times) for the rate than for the corresponding displayed variable itself. i.e., position or pitch angle (Figure 7).

With no predictor, the inner loop (see Figure 1) demands more attention (by about 4 times more than the outer loop), when rate u is not available (cases B C). With the addition of the predictor, position or pitch or their derivatives require comparatively less attention than the predicted variables. The predictor requires 3 to 15 times more attention.

Total attention for the position predictor is about 2 to 3 times greater than that for the pitch predictor (Figure 9). From this and the discussions for RMS-errors, the importance of the position predictor information is obvious.

It should be pointed out that for constant total attention, the RMS-errors are still small even when the information available is limited (e.g., only 3 variables in case I compared to 8 in case L), as long as the position predictor is available. This could be due to less noise in observing what is available and, hence the possibility for better state estimation. From the foregoing discussions it is clear that the rate

information is highly useful when a predictor is not available. Having a predictor for the low speed outer loop is more important for performance since it reduces the RMS-errors more effectively.

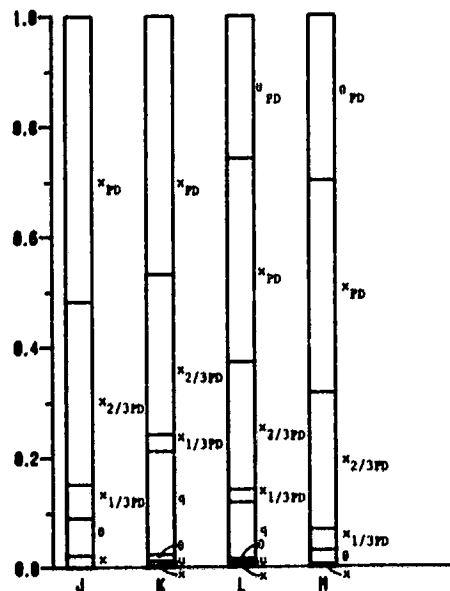


Figure 9: Optimized Fractions of Attention for Cases J,K,L,M

In Figure 10, the RMS-values of position, pitch angle, and control for different cases with and without rate and predictor information are plotted corresponding to optimized attention allocation. These cases have been chosen because the additional indication of the end point of the extrapolated path element (h) compared with the baseline display format (A) results in the simplest predictor display design with the maximum performance improvement. Compared with these two cases, C and I show the influence of the omitted rate information. The trends discussed earlier are seen again in Figure 10.

The effects of varying the total attention and optimizing the attention allocation are illustrated for RMS-longitudinal errors for the cases A,C,H, and I (Figure 11). The first bar in each case corresponds to variable total attention split equally among displays (1 for each observed variable). For the second bar, total attention is 4, split equally between the inner loop and the outer loop, and equally among displays in any particular loop. The remaining bar corresponds to a total attention of 4, split optimally. The errors are reduced by 18% for case A. For case C, a reduction of about 30% occurs when total attention changes from 2 to 4. Optimization reduces this further by only 8%. The slight increase of RMS-error in case H is due to a decrease in total attention from 5 to 4. However, in case I, the increase in total attention from 3 to 4 does not change the RMS-value. When attention is optimized, up to 30% reduction in error is obtained.

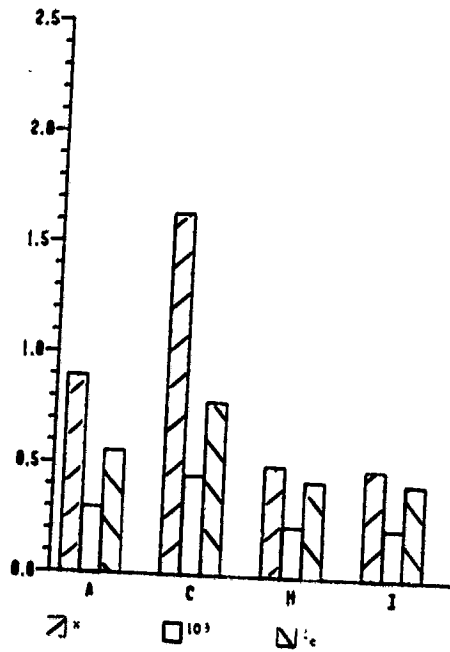


Figure 10: RMS-values of Position x , Pitch Angle θ , and Control δ_c for Cases A,C,H,I with Optimized Attention Allocation.

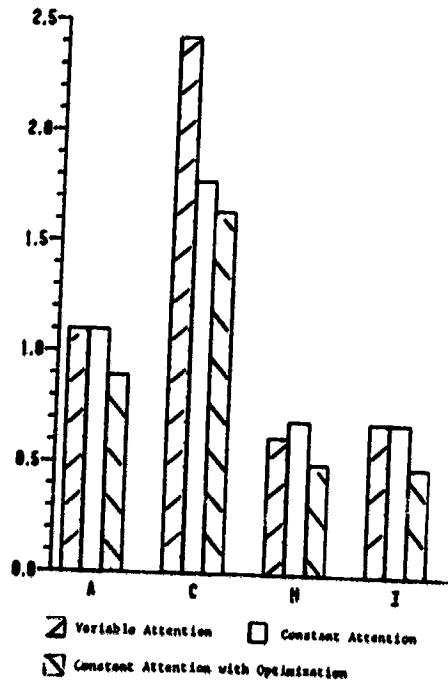


Figure 11: RMS-Longitudinal Errors For Cases A,C,H,I with Variable and Constant Total Attention.

It is necessary to point out that the fractions of attention obtained may not be the globally optimum values. Due to the coupling between inner and outer loop and the interdependence of prediction and rate information (see Figure 2 and Equations 2 and 3), different combinations of initial conditions lead to different optimal attention allocations with similar total cost values. This corresponds, however, to the freedom the human operator has also in choosing between equally appropriate combinations of interrelated information. The optimized fractions of attention shown in this paper seem to be typical values found with different initial conditions.

VI Conclusions

Predictors improve man-machine system performance as shown by the model results of this study. This is consistent with the results obtained e.g., in [5]. The position predictor display is more useful in reducing the RMS-errors. Especially, the end point of the extrapolated path element has the strongest influence. Due to slower dynamics, it is possible that the human finds it difficult to infer the longitudinal position rate compared to pitch rate.

The addition of a predictor might result in reduced workload as evidenced by the smaller RMS-control movements. The control actions by the pilot are guided by the predictor. This could also have an effect on the internal model because estimation of the states is aided by the predictor display. The accuracy requirements of the state predictor implicitly included in the optimal control model of the human operator might be relaxed. The improvement of state estimation with an even inaccurate internal model might also be important for monitoring and supervisory control tasks. Separate studies are needed to evaluate this effect.

The study shows that the optimal control model is suitable for analytical predictor display designs. Using this methodology it is possible to investigate the effects of certain display parameters, e.g., to find the optimal length of the prediction span. This may allow one to avoid expensive man-in-the-loop simulation studies.

VII References

- 1 Wierwille, W.W.; "Improvement of the Human Operator's Tracking Performance by Means of Optimum Filtering and Prediction," IEEE Trans. Human Factors in Electronics, Vol. HFE-5, 1964, pp. 20-24.
- 2 Bernotat, R.: "Das Prinzip der Voranzeige und seine Anwendung in der Flugführung." Z. Flugwiss., Vol. 13, 1965, pp. 373-377.
- 3 Kelley, C.R.; Manual and Automatic Control, New York: Wiley, 1968.
- 4 Warner, J.D.S.; "A Fundamental Study of Predictive Display Systems." NASA CR-1274, 1969.
- 5 Dey, D.; and Johannsen, G.: "Anthropotechnische Untersuchung einer Übergrundanzeige und eines künstlichen Horizonts mit Voranzeige zur manuellen Regelung von VTOL-Flugzeugen," Z. Flugwiss., Vol. 21, 1973, pp. 140-145.
- 6 Roscoe, S.N.; and Eisele, J.E.: "Integrated Computer-Generated Cockpit Displays," In: Sheridan, T.B., Johannsen, G. (Eds.) Monitoring Behavior and Supervisory Control, New York: Plenum Press, 1976, pp. 39-49.
- 7 Machover, C.; Neighbors, M.; and Stuart, C.: "Graphics Displays," IEEE Spectrum, Vol. 14, 1977, pp. 24-32.
- 8 Kleinman, D.L.; Baron, S.; and Levison, W.H.: "An Optimal Control Model of Human Response. Part I: Theory and Validation," Automatica, Vol. 6, 1970, pp. 357-369.

- 9 Johannsen, G.; Boller, H.B.; Donges, E.; and Stein, W: Der Mensch im Regelkreis - Lineare Modelle, München: Oldenbourg. 1977.
- 10 Earon, S.; and Levison W.H.; "An Optimal Control Methodology for Analyzing the Effects of Display Parameters on Performance and Workload in Manual Flight Control", IEEE Trans. Syst. Man Cybern., Vol. SMC-5, 1975, pp. 423-430.
- 11 Earon, S.; and Levison, W.H.; "Display Analysis with the Optimal Control Model of the Human Operator," Human Factors, Vol. 19, 1977, pp. 437-457.
- 12 Hess, R.A.; "Analytical Display Design for Flight Tasks Conducted Under Instrument Meteorological Conditions," IEEE Trans. Syst. Man Cybern. Vol. SMC-7, 1977, pp. 453-462.
- 13 Curry, R.E.; Kleinman, D.L.; and Hoffman, W.C : "A Design Procedure for Control/Display Systems," Human Factors, Vol. 19, 1977, pp. 421-436.
- 14 Miller, D.P.; and Vinje, E.W.; "Fixed-Base Flight Simulator Studies of VTOL Aircraft Handling Qualities in hovering and Low-Speed Flight," Wright-Patterson AFB, Ohio: AFFDL-TR-67-152, 1968.
15. Baron, S.; and Kleinman, D.L.: "Prediction and Analysis of Human Performance in a VTOL Hover Task," Proc. 7th Annual Conf. on Manual Control, NASA SP-281, 1972, pp. 247-256.
- 16 Hess R.A., "Prediction of Pilot Opinion Ratings Using an Optimal Pilot Model," Human Factors, Vol. 19, 1977, pp. 459-476.
- 17 Earon, S.; and Berliner, J.E.; "The Effects of Deviate Internal Representations in the Optimal Model of the Human Operator." U.S. Army Missile Research and Development Command, Alabama: Tech. Rept. TD-CR-77-3, 1977.
- 18 Curry, R.E.; Hoffman, W.C.; and Young, L.R.; "Pilot Modeling for Manned Simulation," Vol. I; Doyle K M and Hoffman W C, ..., Vol. II (Program User's Manual), Wright-Patterson AFB, Ohio: AFFDL-TR-76-124, 1976.
19. Hoffman, W.C.; Curry, R.E.; Kleinman, D.L.; Hollister, W.M.; and Young, L.R.; "Display/Control Requirements for VTOL Aircraft," Aerospace Systems, Inc. Burlington, Mass : ASI-TR-75-26 (NASA CR-145026), 1975.